Kinetics of Lead Release from Brass Water Meters and Faucets

(presented at American Waterworks Association Water Quality Technology Conference, 2008)

J. Barry Maynard, Ph.D and **David Mast, Ph.D** University of Cincinnati, 500 Geology/Physics Bldg, Cincinnati OH 45221
Pierre Kwan, PE, HDR Engineering, 500 108th Avenue NE, Suite 1200, Bellevue, WA 98004-5549

With contributions by
Jim Dunn and Brian Hoyt (retired), Seattle Public Utilities, Water Quality Laboratory, 800 S. Stacy Street, Seattle, WA 98134
Yone Akagi, PE, Portland Water Bureau, 1900 N. Interstate Avenue, Portland, OR 97227

Abstract

As part of AwwaRF project 3018, the release of Pb from new brass kitchen faucets and new and used brass residential-service water meters was measured. Data were obtained for brass compositions, scale compositions, and water chemistry. Pb (or Bi) is present in these brasses as small "islands" of metal, whereas Cu and Zn are mixed in a solid solution. With time, Zn in the brasses was preferentially lost relative to Cu.

Pb releases from the brass faucets in 6 hour stagnation runs increased rather than decreased with time. This behavior is inconsistent with formation of passivating scale layers, but is consistent with progressive dezincification producing a porous surface layer through which Pb can diffuse more rapidly, or from which Pb particulates can be detached more readily with time. The rate of Pb release was found to correlate inversely with the Zn/Cu ratio of the brass.

Metal release rates from meters could be effectively modeled as controlled by two processes. Initially, the release curves for Cu, Zn, and Pb follow $t^{1/2}$ kinetics, indicating that the reaction is transported limited by diffusion. At longer times, the reaction rate follows first-order kinetics consistent with consumption of oxygen as the rate limiting step. Rate constants for the first stage correlate to the age of the meters, whereas for the second correlate to the Zn/Cu ratio – higher Zn brasses corrode more slowly. This relationship is likely caused by autocatalyic oxidation of copper via

$$Cu\ metal + Cu^{2+} \rightarrow 2Cu^{1+}$$

As long as oxygen remains in the water, the cupric ions can be regenerated via

$$4Cu^{1+} + 4H^+ + O_2 \rightarrow 4Cu^{2+} + 2H_2O$$
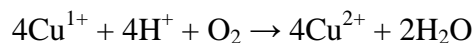
and the reaction continues. The higher Cu brasses (those with lower Zn/Cu ratios) release more Cu to solution in short stagnation cycles; therefore they corrode more quickly than lower Cu brasses. In flowing water, the buildup of the copper ions in solution is

precluded, and the autocatalytic effect does not occur. In this case, the corrosion rate is controlled by the diffusion of Zn (and Pb) from the metal, which should increase with increasing Zn content.

Introduction

Water distribution systems and household plumbing contain numerous brass components. Most such components in service are leaded brass and hence comprise a potential source of Pb in compliance testing under the Lead and Copper Rule. For households, the two components with the greatest internal volume and hence the greatest potential to affect the Pb content in tap water are faucets and meters. Of the two, faucets are directly at the site of testing and hence are more likely to be represented in LCR compliance samples.

Typical brasses used in these applications are alloys of Cu, Zn, and Pb with small amounts of other metals such as Sn. The Pb content is typically 2 to 8 %, and is not uniformly present in the alloy but as discrete blebs. In no-lead brasses, Bi and Se are used instead, and also occur in these blebs. The addition of Pb or Bi is made to improve the machinability of the brass. Imaging using Scanning Electron Microscopy (SEM) reveals this structure (Fig. 1). The image was taken in back-scatter mode, in which the brightness is proportional to the atomic number of the element. The large contrast in mass between Pb and the other elements produces the bright spots. Note also the porous zone at the wetted edge of the brass revealed by the dark areas.
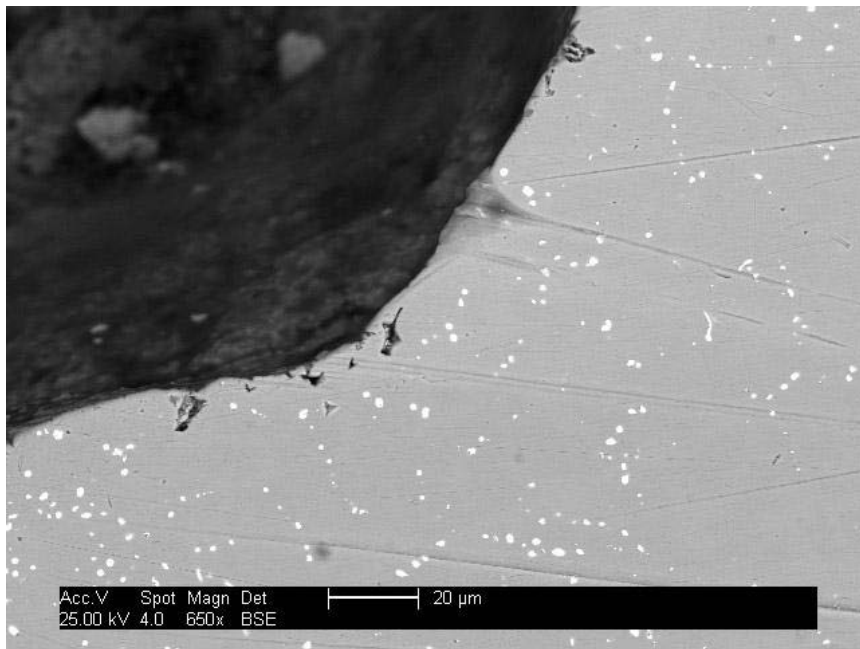

Figure 1. Structure of brass revealed in SEM imaging, using back-scattered electrons. Polished section cut through a leaded brass faucet.

Six new faucets and six meters of a variety of ages were incorporated in automatic rigs to simulate daily household use over an extended time frame, For the faucets, the time frame was 13 months in a rig installed at the Portland Water Bureau, while the meters were used for 6 months at Seattle Public Utilities.

Faucet stagnation experiments

Six faucets from the Portland faucet rig experiment (Kwan et al., 20__) were tested for scale development and for effects of leaching on metal compositions. Two of the units tested were replicates — Faucets 1 and 2. Metal composition of the faucets before being placed in the rig was determined by analysis of duplicate samples by the Copper Development Association (Table 1).

Table 1. Metal contents of faucets used in scale analysis.					
Faucet	Internal Wetted Vol., ml	Average Pb %	Average Cu %	Average Zn %	Zn/Cu Ratio
1	201	2.43	57.7	38.9	0.67
2	201	2.43	57.7	38.9	0.67
3	171	2.13	57.6	39.1	0.68
4	134	0.08	91.5	4.2	0.05
5	162	2.35	57.8	38.0	0.66
6	95	2.87	57.7	37.2	0.65
Averages calculated from analyses of lower and upper valve body plus spout receiver, excluding spout					

ANSI/NSF 61 Testing

Additional duplicates of the faucets used in the scale study were tested using the ANSI/NSF 61 protocol (Table 2). Faucets 1 and 2 exceeded the Pb limit of 11 µg/L. Amounts of Cu and Zn are also available from this test. The high ratios of Zn to Cu in the leachate compared to the ratios in the metal indicate strong dezincification of the brass in these faucets in the test procedure.

Table 2. Metal release results from NSF 61 testing						
Faucet	Internal Wetted Vol., ml	NSF 61 Pb Q (µg/L)	NSF 61 Cu (µg/L)	NSF 61 Zn (µg/L)	Zn/Cu	Zn/Cu$_{leachate}$/ Zn/Cu$_{solid}$
1	201	18	11	91	8.3	12
2	201	18	11	91	8.3	12
3	171	11	2	160	80	118
4	134	11	14	84	6.0	128
5	162	2.7	2.9	71	24	36
6	95	1.7	.3	58	190	292

Water chemistry

The water quality parameters alkalinity, pH, and temperature were measured for each faucet. Other parameters were available for the source water from the Portland Water Bureau annual water quality reports (Table 3). Equilibrium modeling of this water chemistry incorporating measured Pb concentrations (Table 4) showed that the only Pb

Table 3. Portland water chemistry	
Temperature (^oC)	15.5
pH (specific units)	8.1
Alkalinity (as CaCO3)	13
SO4	0.25
Cl	2.4
Na	4.1
Fe	0.087
Al	0.03
Ca	0.8
Mg	0.8
Mn	0.011
Si	4.7
K	0.2
P	0.014
units of concentration are mg/L unless noted otherwise	

mineral supersaturated with respect to the water was pyromorphite ($PbPO_4$). The mineral next closest to saturation was cerussite ($PbCO_3$) but it is always somewhat undersaturated.

In Table 4, Pb releases measured in the faucet rig are compared to those measured using the NSF 61 procedure. The results suggest that the NSF protocol is not a good predictor of long-term behavior of brass faucets. See Dudi et al. (1997) for a critique of this procedure. Note also in Table 4 that the first 100 ml contains most of the Pb released, that there is a wide variability in the amounts of Pb released and also that the replicate faucets 1 and 2 released quite different Pb amounts.

Table 4. Summary of Pb results for Portland faucet rig			
	1st liter	1st 100 ml	NSF 61
Faucet	Pb, µg/L	Pb, µg/L	Pb Q (µg/L)
1	1.03	6.03	18
2	0.75	3.83	18
3	0.50	2.19	11
4	3.65	13.14	11
5	1.82	9.90	2.7

| 6 | 1.36 | 5.62 | 1.7 |

Pb concentrations are averages of 18 sequential draws over one year of operation of faucets; no Zn or Cu measurements were made.

Scale Development

None of the faucets showed extensive scale development. That is, passivating scales did not form over the 13-month experimental period, although in some cases small patches of scale did form. Instead, the dominant process is the formation of a Zn-depleted layer on the internal surfaces of the faucets. This process is most easily seen with Faucets 1 and 2 (Fig. 2 and 3).
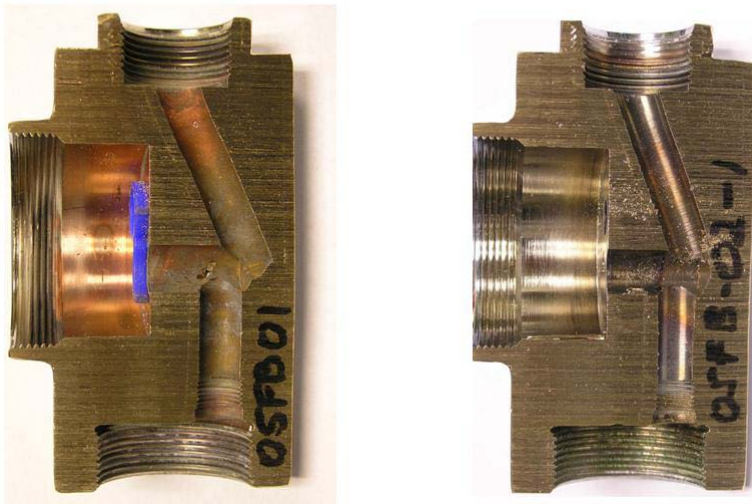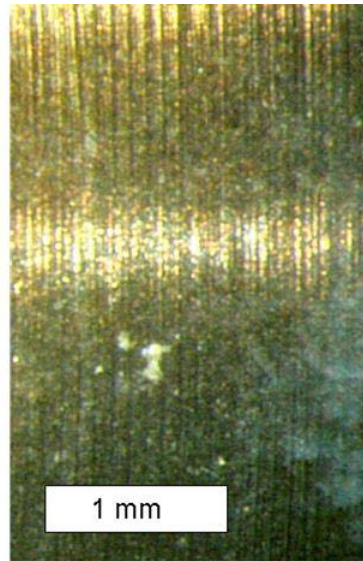

Figure 2. Cut sections through the valve body for Faucets 1 and 2. Although identical designs from the same manufacturer, behavior is quite different. FB01 has a well-developed copper color, indicating dezincification, whereas FB02 largely retained its original yellow brass color.
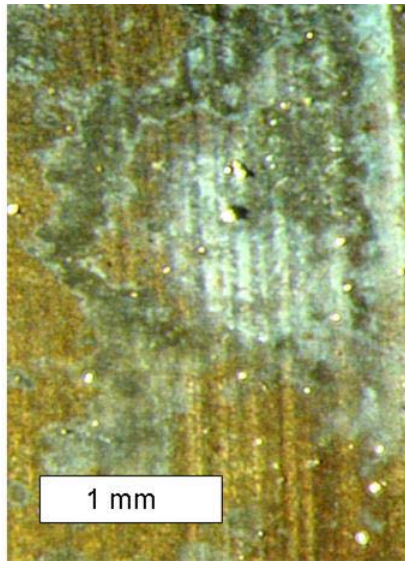
FB01   **FB02**

Figure 3. Photomicrographs of the valve body for Faucets 1 and 2 show spotty scales in both, but heavier coverage in FB01.

Dezincification of the brass can be imaged using the back-scattered electron technique (Fig. 4 and 5). In the scans below, Pb-rich regions are very bright, normal brass is gray, and Zn-depleted brass is dark gray. Note that the Cu and Zn form a solution, but that the Pb component remains as isolated, distinct nodules a few tenths of a micron across.
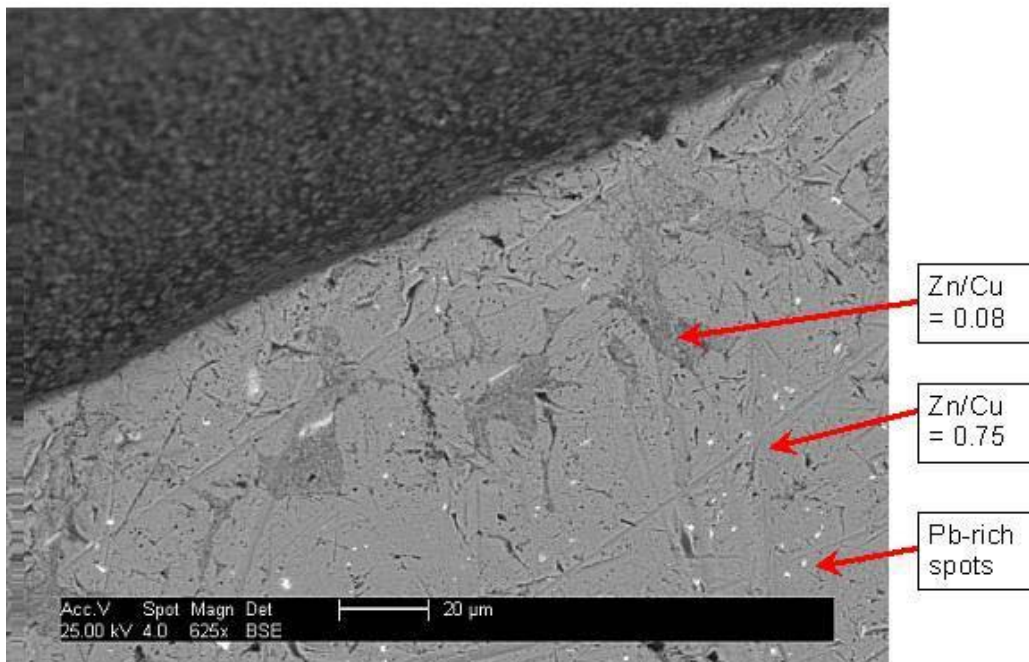
05_FB01 Brass faucet

Figure 4. Back-scatter image of the edge of the brass along an interior surface of Faucet 1. A zone a few microns thick at the surface has developed that is both depleted in Zn and more porous (shown as the black voids) than the bulk metal.
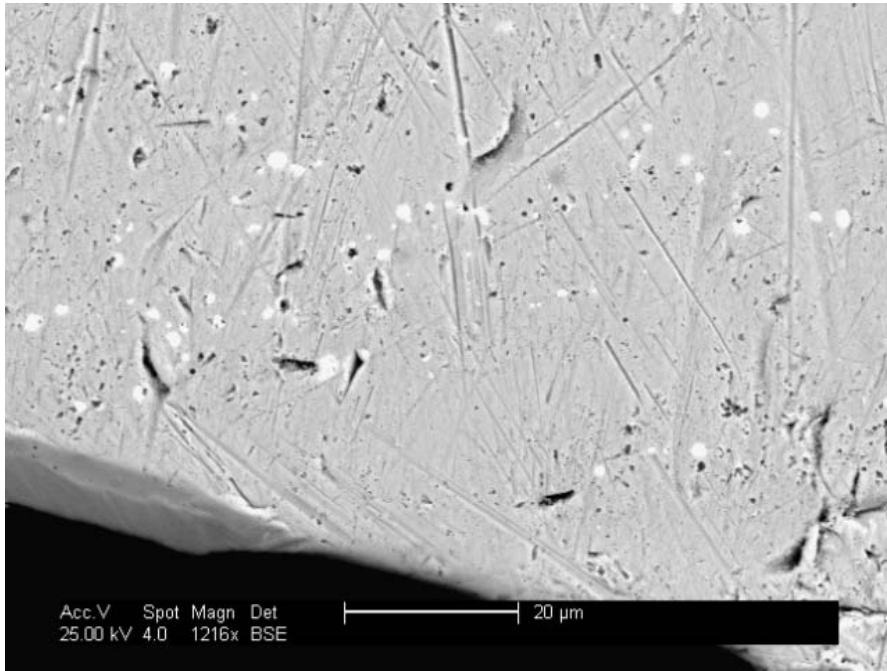

Figure 5. Back-scatter image of the edge of the brass in Faucet 2. Note the lack of a porous, Zn-depleted area along the surface.

The brass in the two versions of this faucet used in the rig was in fact slightly different. Energy dispersive analysis (EDS) in the SEM showed Zn/Cu to be 0.75 in Faucet 1, whereas in Faucet 2 it was 0.92. Thus Faucet 2 has higher Zn than its twin, showing the range of variability in manufacturing. Furthermore, it would appear that the higher Zn faucet is *less* susceptible to dezincification.

Dezincification was also seen extensively developed in Faucet 4. Back-scatter imaging of the spout from this faucet shows severe dezincification that underlies organic-rich crusts on the brass, consistent with a microbial role in the brass corrosion (Fig. 6 and 7). See Valcarce et al. (2005) for a discussion of such microbial effects in brass corrosion.
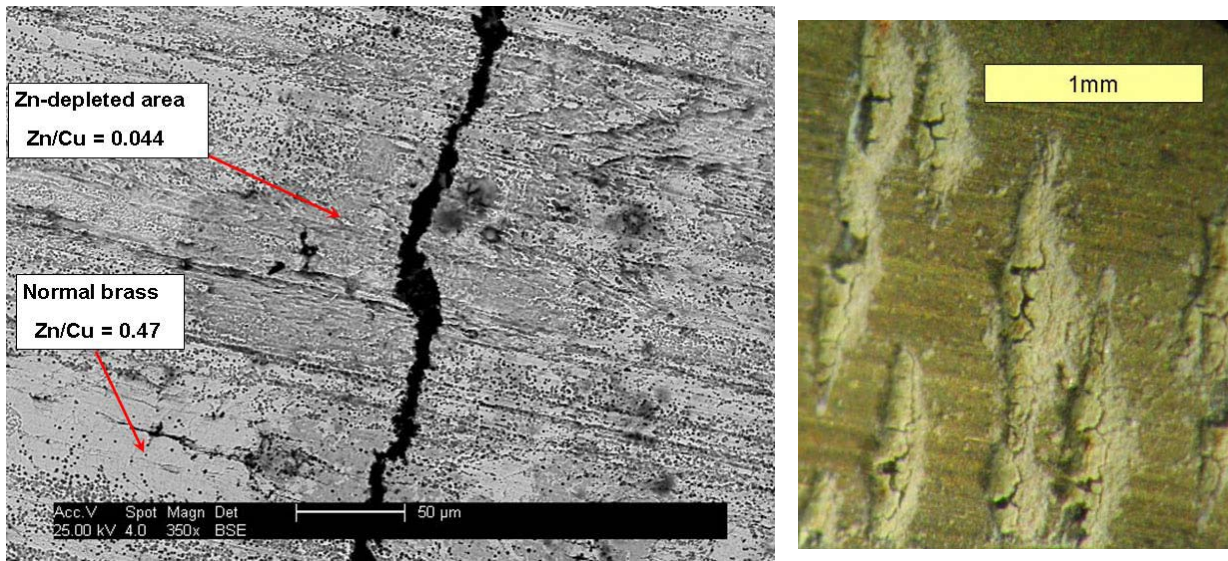
Figure 6. Back-scattered electron image of spout. Tension cracks from shaping the spout have become localized areas of corrosion. There is a marked dezincification along all of these cracks -- bright areas are zinc-rich, normal brass; gray areas are zinc-depleted. When received, these cracks were covered by a fragile, organic-rich accumulation, likely microbial in origin, shown on the right.
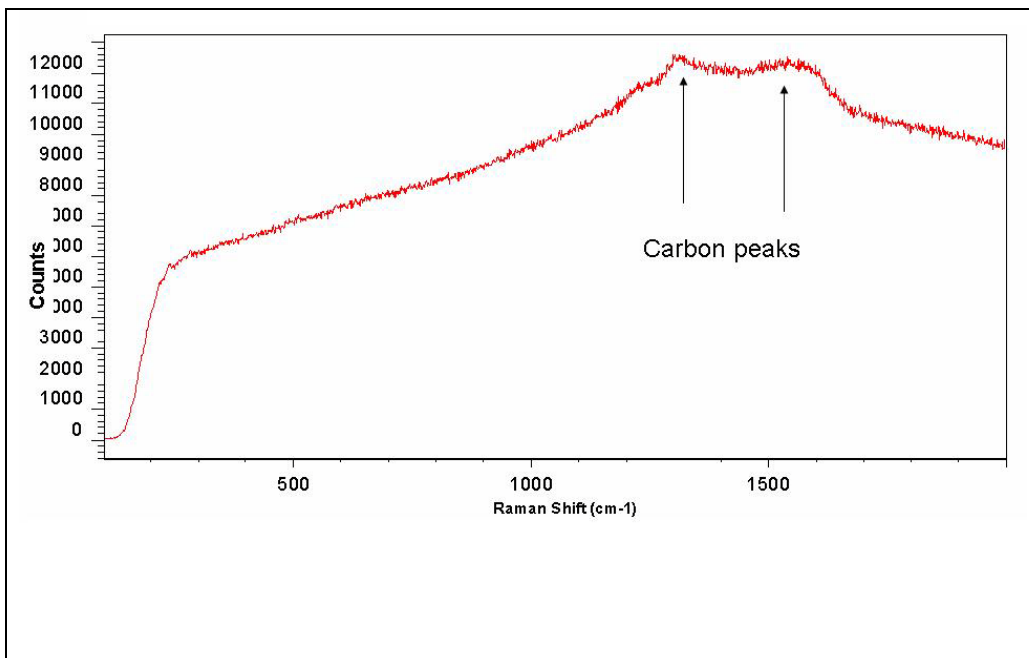

Figure 7. Raman spectrum of ridges on spout interior surface. These ridges or mounds cover tension cracks; the Raman signal confirms that these are organic in origin.

Faucet 4 also showed the heaviest scale buildup on the valve body. This scale comprises mostly Cu carbonates, but many areas show a surprisingly high zinc concentration in the form of a ZnO mineral (Fig. 8).
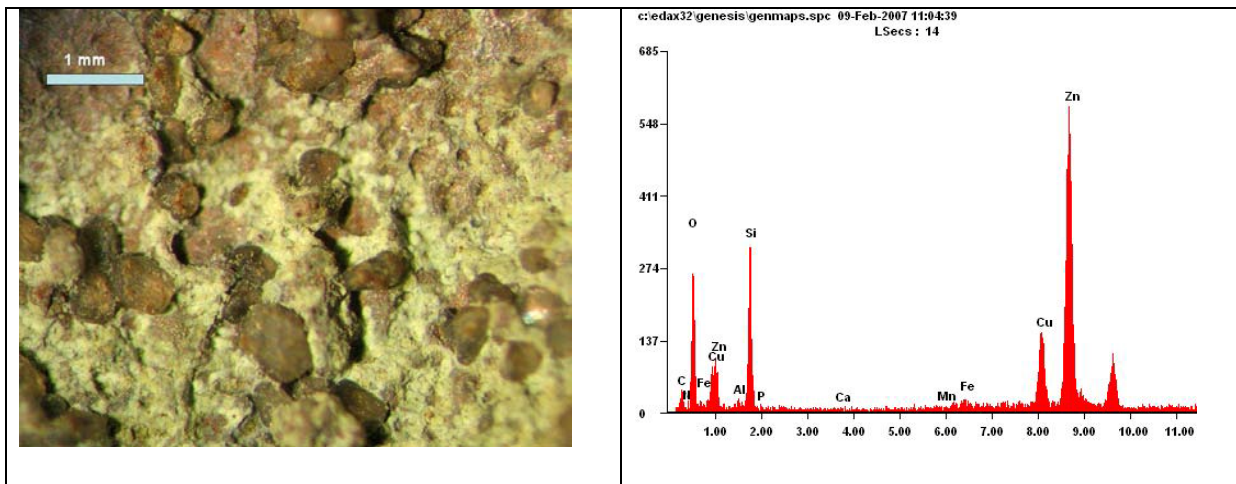

Figure 8. Photomicrograph of interior of the spout holder (left) and EDS spectrum from the white portion of the scale (right). The large brown grains in the photograph are sand grains left from the original casting of the brass. They are partly surrounded by greenish scale (Cu carbonate) and whitish scale (ZnO). The Si in the spectrum is from quartz in the sand. Note also a small amount of Fe-Mn oxide, which imparts a brown stain to the quartz grains.

A peculiar situation was discovered in the analysis of the valve parts in Faucet 4. This unit was marketed as Envirobrass, in which Bi is used to replace Pb. Analysis of a duplicate faucet showed Pb contents to be quite low, ranging from below detection to 0.01 %. SEM-EDS analysis of the movable valve parts, however, showed high Pb and no Bi. These results were confirmed by X-ray fluorescence analysis of the parts.

Faucets 3, 5, and 6 showed no obvious scale development and had no obvious dezincification features.

Comparison of brass corrosion features to water chemistry results

Lead releases from the faucets, as determined in sequential sampling after 6 hour stagnation, tended to increase rather than decrease with time (Table 5). This behavior is inconsistent with formation of passivating scale layers, but is consistent with progressive dezincification producing a porous surface layer through which Pb can more readily diffuse out as dissolved Pb, or be detached more readily as particulate Pb, with time.

In Table 5, Pb, Cu, and Zn contents of the actual faucets tested, as determined by energy-dispersive spectroscopy, are also given. Using these values, there is a correlation between Pb content of the faucets and the amount of total Pb released. The relationship, however, is based only on the high Pb content of the valve in Faucet 4 (Fig. 9). There is also,

however, a correlation with the Zn/Cu ratio of the brass, which shows a distribution across all the faucets (Fig. 10).

| Table 5. Pb extracted during sequential sampling, one liter aggregate sample						
	Faucet 1	Faucet 2	Faucet 3	Faucet 4	Faucet 5	Faucet 6
Date	µg Pb	µg Pb	µg Pb	µg Pb	µg Pb	µg Pb
10/20/2005	1.34	0.74	0.21	2.65	0.98	0.57
10/24/2005	1.52	1.16	0.21	0.39	0.86	0.51
10/27/2005	1.34	0.75	0.21	0.45	0.92	0.50
10/31/2005	1.28	0.92	0.27	0.39	0.92	0.45
11/7/2005	1.16	0.74	1.11	0.39	0.74	0.62
11/14/2005	2.54	0.62	0.15	0.27	0.68	0.39
1/12/2006	1.04	0.44	0.15	0.33	0.74	0.33
1/26/2006	0.86	0.33	0.27	1.71	0.44	0.44
2/9/2006	0.68	0.33	0.15	0.21	0.44	0.27
2/23/2006	0.68	0.27	0.27	0.21	0.39	1.71
3/23/2006	0.50	2.06	1.18	33.24	2.18	2.54
4/20/2006	0.39	0.21	0.15	8.26	0.44	0.44
5/18/2006	3.06	3.24	3.12	5.98	4.12	5.02
6/15/2006	0.38	0.32	0.21	0.45	0.21	0.33
7/24/2006	1.01	0.33	0.39	2.44	0.33	2.39
8/17/2006	0.33	0.50	0.21	0.33	16.10	2.02
9/7/2006	0.33	0.39	0.45	0.10	1.94	0.80
10/5/2006	0.68	0.45	0.50	8.72	1.89	5.90
11/2/2006	0.50	0.39	0.27	2.85	0.27	0.63
Avg. Pb, µg	1.03	0.75	0.50	3.65	1.82	1.36
Faucet %Pb	1.62	1.62	1.85	[1]5.59	2.35	2.17
Faucet Zn/Cu	0.75	0.92	0.67	0.47	0.65	0.64
[1]SEM_EDS of valve used for Pb %						
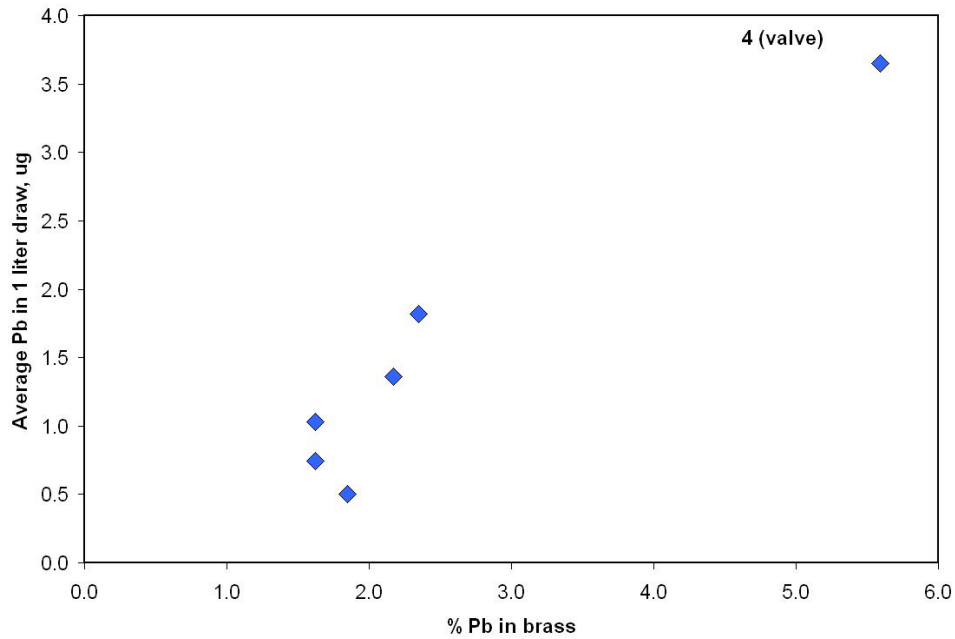
Figure 9. Rate of total Pb release as a function of Pb content of brass. The value for Faucet 4 is taken from the valve only; the rest of the faucet is < 1% Pb.
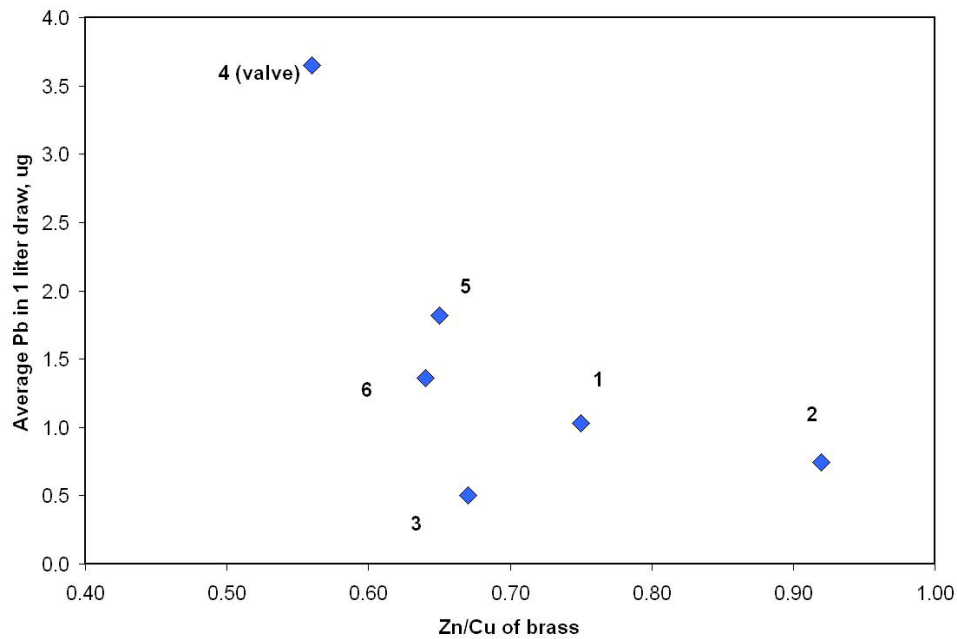

Figure 10. Rate of total Pb release as a function of Zn/Cu content of brass. The inverse relationship with Zn content is unexpected, but is shown dramatically by faucets 1 and 2, which are identical in all other aspects.

Seattle meter rig

Six ¾-inch residential-service brass water meters were used in side-by-side testing to identify their potential Pb and Cu contributions to water in first-draw stagnation samples. The meters ranged in service age from new, never used units to one that had been in service for 40 continuous years. Five of the meters were brass with up to 8% Pb content, and one was the new "no-lead" brass in which the Pb content is less than 0.2%, and Bi and Se (a regulated element in drinking water) are used in its place (Table 6). A seventh meter, which was not used in the rig, was tested as received out of the box.

| Table 6. Metal contents of meters determined before insertion in rack										
			Metals Concentration							
Meter #	Manufacturer	Age of Meter	% Pb	% Cu	%Zn	%Se	%Sb	%Bi	%Fe	Zn/Cu
1	A	26 yr.	4.97	83.64	4.52	0.037	0.064	0.000	0.131	0.0540
2	B	19 yr.	6.83	80.12	7.91	0.000	0.081	0.000	0.178	0.0987
3	B	4 yr.	7.01	80.86	8.77	0.000	0.035	0.000	0.195	0.1084
4	C	40 yr.	6.45	79.42	9.60	0.000	0.000	0.000	0.096	0.1208
5	D	New	0.03	90.01	5.69	0.325	0.000	1.726	0.000	0.0632
6	B	New	6.65	78.97	8.19	0.000	0.000	0.086	0.221	0.1038
7	B	New, unused	6.65	78.97	8.19	0.000	0.000	0.086	0.221	0.1038
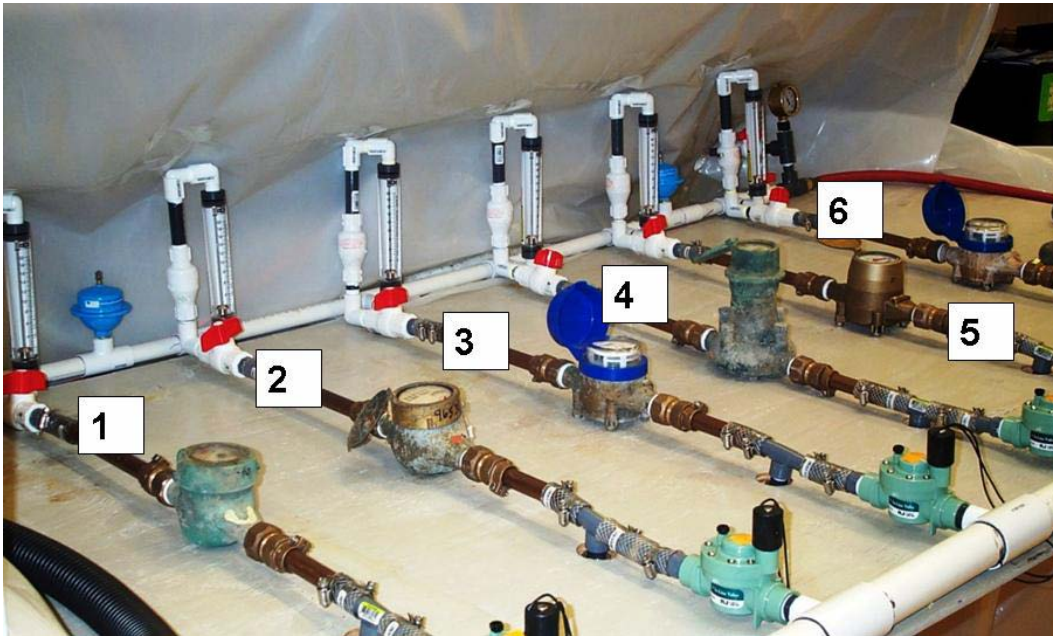
Figure 11. Water meter test rig. Meter 7 was not installed in the rig.

Input water quality

The meter rig used drinking water from Seattle's Cedar River supply. Input parameters for the rig are shown in Table 7, based on laboratory measurement of the water coming in to the rig for pH, alkalinity, temperature, lead, copper, and selenium. Other parameters are from the utility's 2005 water quality reports.

Table 7. Water quality of input water for Seattle meter rig.		
pH	8.24	Standard units
Temperature	10.9	Degrees C
Alkalinity	21.7	mg/l as $CaCO_3$
Chloride	4.7	mg/l
Sulfate	1.4	mg/l
Fluoride	0.95	mg/l
Phosphate	0.004	mg/l
Nitrate	0.055	mg/l
Sodium	2.76	mg/l
Potassium	0.27	mg/l
Magnesium	1.11	mg/l
Calcium	10.08	mg/l
Iron	0.036	mg/l
Manganese	0.004	mg/l
Lead	0.00049	mg/l
Copper	0.0322	mg/l
Selenium	0.00011	mg/l

These data can be used to predict what scale minerals are likely to form in the Seattle distribution system. Using the PHREEQC model from the US Geological Survey with the MINTEQ database option (Table 8), none of the common Pb minerals is stable when exposed to the water quality conditions in the Cedar drinking water. Cerussite, common as a scale mineral in other drinking water systems, is significantly undersaturated, and the distribution water can be expected to be aggressive to any pre-existing Pb carbonates. Several Fe and Mn oxide minerals are supersaturated, as is the Cu oxide tenorite and the carbonate malachite. These minerals are likely to be important components in scales formed in Seattle distribution materials. The Al hydroxide gibbsite is slightly supersaturated, and could precipitate.

Table 8. Saturation states from PHREEQC speciation model using MINTEQ database		
Mineral	Formula	Saturation Index
Cerussite	$PbCO_3$	-2.04
Gibbsite	$AlOH_3$	0.53
Goethite	$FeOOH$	5.42
Hydroxylapatite	$Ca_5(PO_4)_3OH$	0.38
Malachite	$Cu_2(OH)_2CO_3$	1.64
Manganite	$MnOOH$	1.21
Pyromorphite	$Pb_5(PO_4)_3Cl$	-2.13
Tenorite	CuO	0.69
The saturation index is the log of the ratio of measured concentrations to equilibrium concentrations. A negative value indicates water compositions undersaturated with the mineral		

Descriptions of Individual Meters

Meter #1.

Meter 1 had been in service for 26 years. Its metal content is 5 % Pb with a Zn/Cu ratio of 0.054. Visually, it is coated with a thin, even film of a white scale with some brown patches (Fig. 12a). In SEM, the scale is seen to consist of Cu oxide with minor Fe oxide, but with abundant siliceous skeletons of diatoms (Fig. 12b). EDS indicates about 2 % Fe and 6 % Si in addition to Cu and Pb. After 20 hours of stagnation, meter 1 had released about 170 µg/l of Cu, 28 µg/l of Zn and 7.5 µg/l of Pb. The Zn release rate is faster than the Cu release rate, indicating preferential dezincification of the brass.
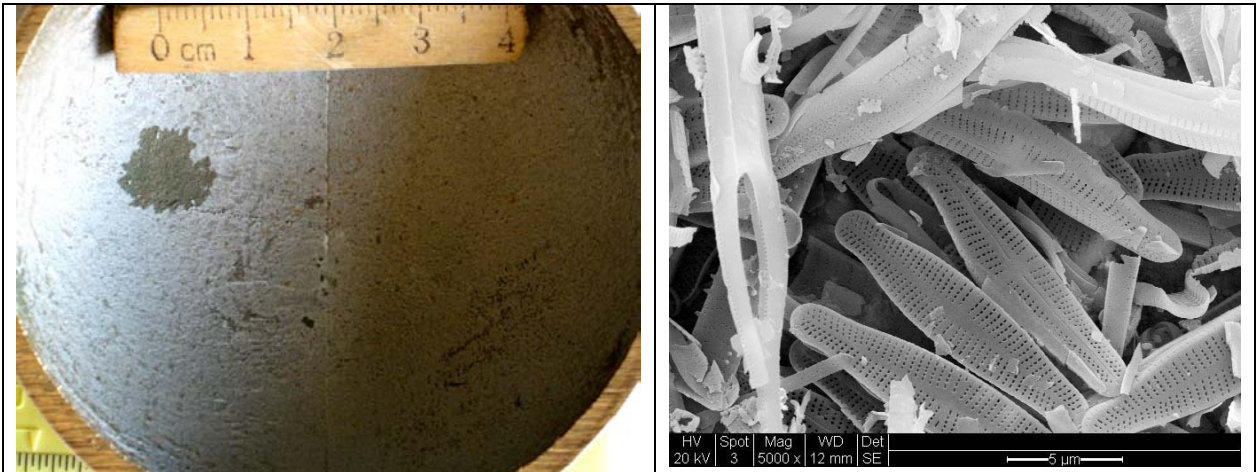

Figure 12. Meter 1. Left: macrophoto of meter bottom. Right: SEM photo showing abundant diatoms.

Meter #2

Meter 2 had been in service for 19 years. Its metal content is 6.8 % Pb with a Zn/Cu ratio of 0.099. Visually, it has a thin, patchy film of white scale with large areas of brass showing through (Fig. 13, left). SEM analysis indicates that this scale is a mixture of Pb and Cu oxides with minor Fe oxide. Pb content is between 20 and 30 %. Fe and Mn are in the 1 to 2 % range (Fig. 13, right). Metal release kinetics for meter 2 are similar in form to meter 1, but Pb release is somewhat slower, as shown in Fig. 13. Cu and Zn release rates are similar to each other, but note that the Zn curve is slightly steeper than the Cu curve at the end of the experiment, again consistent with dezincification of the brass.
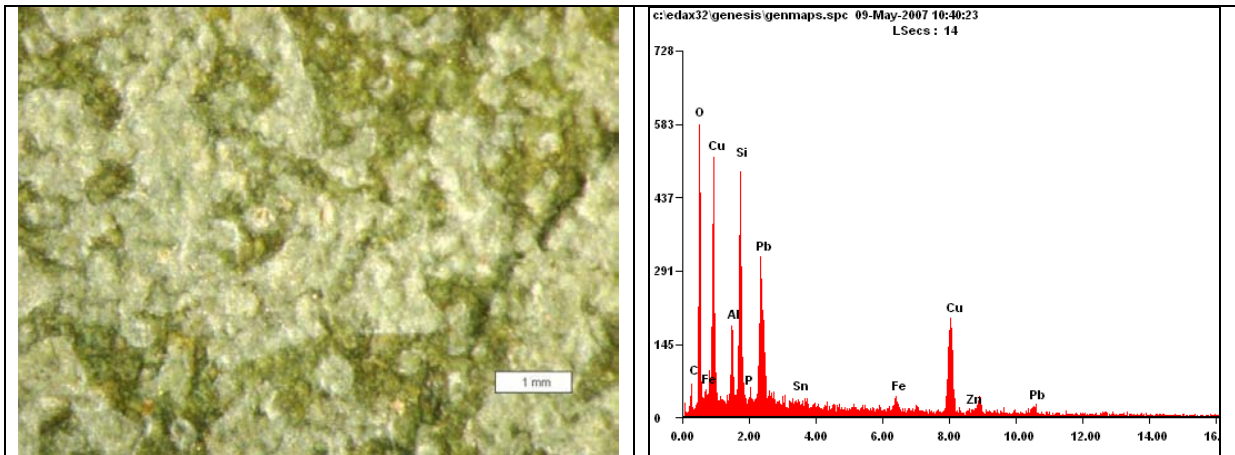
Figure 13. Meter 2. Left: macrophoto showing complete scale coverage. Right: SEM-EDS spectrum showing abundant Pb, Si, and Al in addition to Cu.

Meter #3

Meter 3 had been in service for 4 years. Its metal content is 7 % Pb with a Zn/Cu ratio of 0.11. Visually, it has a few areas with patchy green and white scale. These are best developed in sheltered areas away from the rotor, whose rotation had continually eroded the metal surface where it contacted. SEM analysis shows this material to be Cu oxide and carbonate that contains 15 to 30 % Pb. Fe and Mn are less than 1%. Metal release rates for Pb were somewhat slower than for meters 1 and 2. Cu and Zn rates are similar to each other, but Zn is being leached faster than Cu at the end of the experiment.
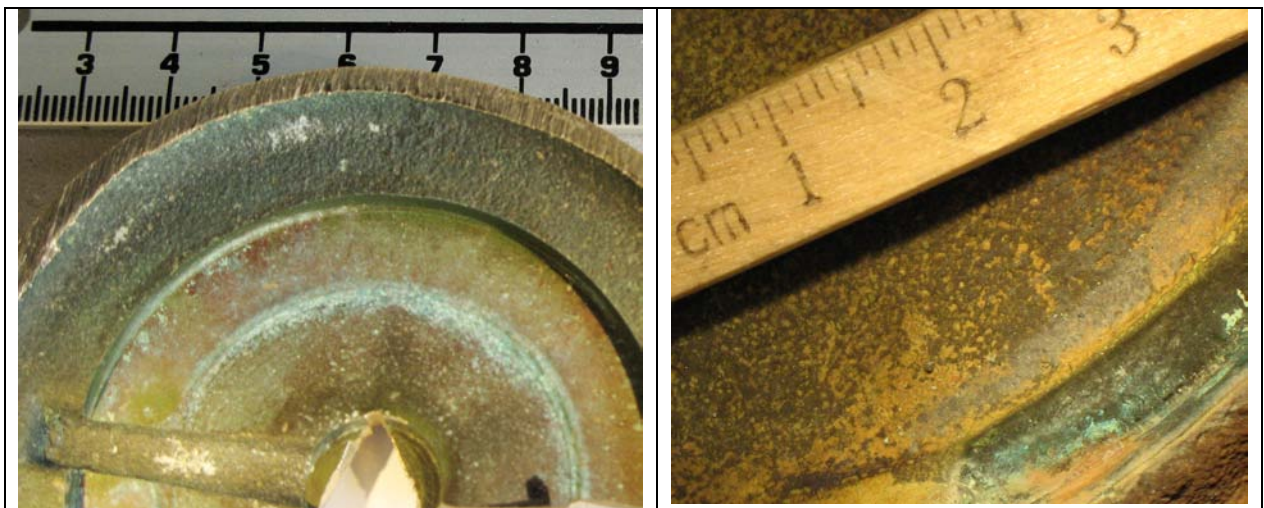

Figure 14. Meter 3 (Left) and Meter 4 (right). Both show wide coverage by Cu oxide (tan) with spotty Cu carbonate (green) and Pb carbonate (white)..

Meter #4

Meter 4 had been in service for 40 years. Its metal content is 6.5 % Pb with a Zn/Cu ratio of 0.12, the highest among the meters tested. Visually, it has extensive areas of thin brown scale with smaller patches of green and white scale (Fig. 14, right). In the SEM, the scale shows an even, granular appearance. EDS analysis indicates about 10 % Pb and 10 % Fe, the Fe most likely as an oxide. Copper in the scale appears to be present as both the oxide and the carbonate. Meter 4 shows considerably lower Pb release than for the previous meters and Cu and Zn release rates are essentially identical, indicating that preferential dezincification is no longer an important process for this aged brass.

Meter #5

Meter 5 was a new meter constructed of Envirobrass, an alloy in which bismuth replaces lead. This meter showed no visible corrosion. Metal release kinetics for Cu and Zn from meter 5 follow a similar pathway to that seen in the other meters. There are also minor amounts of Bi released (up to 0.25 μg/l). Zn release is significantly faster than Cu release, so the envirobrass, like more traditional brasses, is undergoing dezincification.

Meter #6

Meter 6 was a new meter with 6.7 % Pb and a Zn/Cu ratio of 0.103. This meter showed white corrosion deposits at various points on the meter bottom. SEM analysis indicates a Pb carbonate, most likely hydrocerussite (Fig. 15, left). In addition to Pb, the scale only has small amounts of Cu. The Fe and Mn seen in older meters are lacking. Metal release rates for meter 6 show Zn release to be significantly faster than Cu release, so that dezincification is more intense in the newer meters. This meter had the highest Pb concentration after 20 hr stagnation. Based on PHREEQC models, some of this Pb may come from dissolution of Pb carbonate rather than from leaching of Pb from the brass itself.
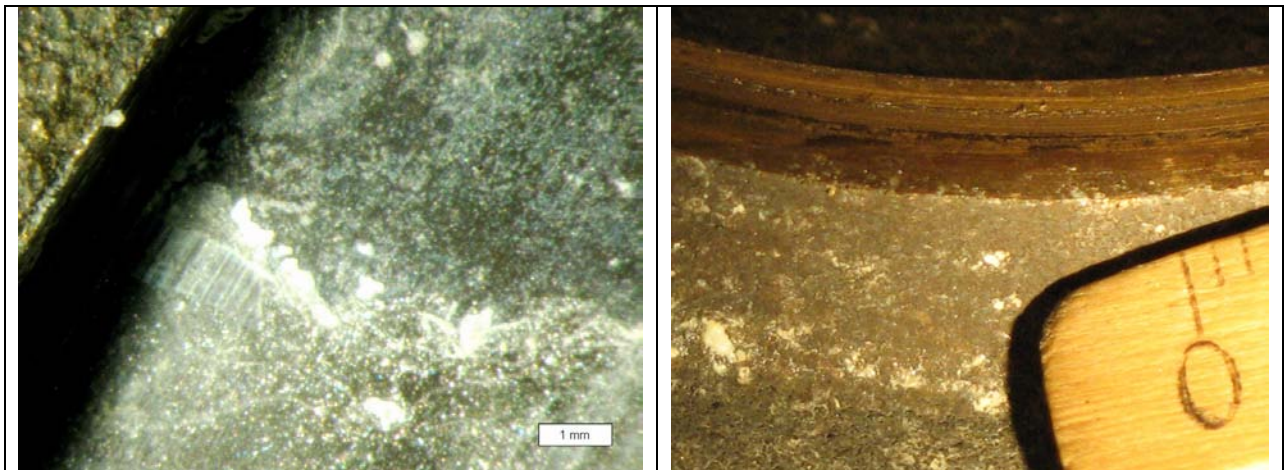
Figure 15. Left: Meter 6 (new), Right Meter 7 (new, never used). The white spots on both are Pb carbonate

Meter #7

The bottom of meter 7, which was never mounted in the rig and thus serves as a blank, has patches of white scale (Fig. 15, right). In the SEM, these patches are seen to be lead carbonate, probably hydrocerussite. The presence of Pb carbonate scale in the blank means that the degree of scale development in the meters is not a useful parameter. The chemical conditions under which these scales developed in unused meters is unknown. However, the undersaturation of the Seattle Cedar supply with respect to both Pb the carbonates (cerussite and hydrocerussite) suggests that these scales will dissolve once the meter is in service and could provide an extra source of Pb.

Kinetics of Reaction in Meter Experiments

The initial reaction progress for each meter can be modeled effectively with a power function of the form

$$y = kt^{1/2}$$

where y is the metal concentration in ppb, k is a rate constant, and t is time in seconds. The $t^{1/2}$ dependency is characteristic of diffusion-controlled kinetics (Crank, 1956) and many corrosion reactions of metals have diffusion as the rate limiting step (e.g. Cardew, 2006). Table 9 gives the initial rate constant for each metal. The rate constant for Zn and for Pb decrease with the age of the meter (Fig. 16).

Table 9. Initial rate constants for leaching of brass meters during stagnation.					
Meter	Age years	$k_{D,Cu}$	$k_{D,Zn}$	$k_{D,Pb}$	Zn/Cu brass
5	0	*1.432*	*0.079*		0.063
6	0	1.354	0.096	0.053	0.103
3	4	1.633	0.078	0.030	0.108
2	19	1.187	0.078	0.021	0.098
1	26	0.892	0.053	0.022	0.054
4	40	1.496	0.058	0.013	0.120
Units of k are $\mu g \cdot L^{-1} \cdot sec^{-1/2}$					

As reaction proceeds, the model overestimates metal concentrations, as shown in Fig. 17. The slowing of the reaction indicates that a different process has become rate limiting. The likely candidate is the rate of oxidation of the metals to their cationic equivalents.
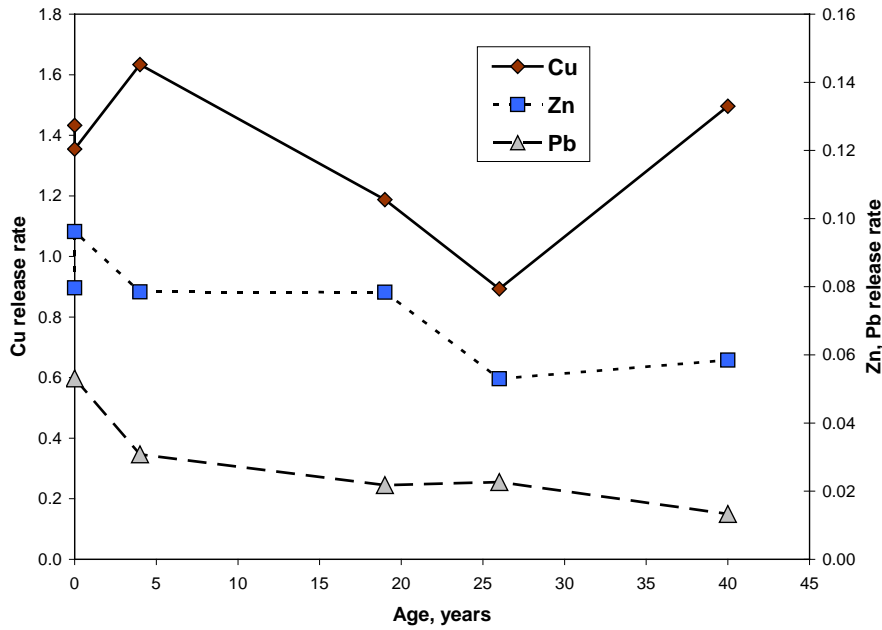
Figure 16. Variation of the initial rate constant with the age of the meter.
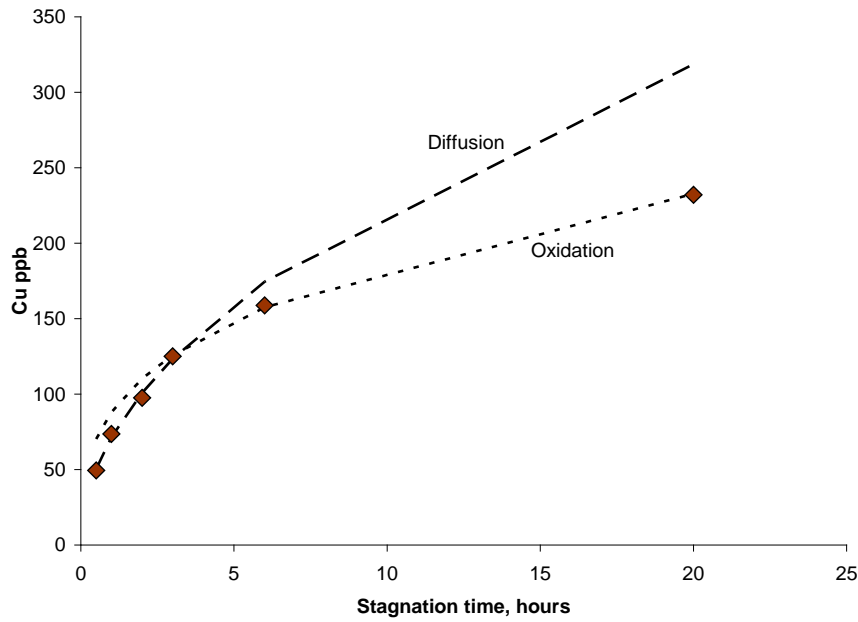

Figure 17. Departure of Cu release rates from diffusion-controlled kinetics at long stagnation times.

According to Merkel et al. (2002), oxygen consumption in copper corrosion follows first-order kinetics. That is the rate is given by

$$[O_{2,t}] = [O_{2,t=0}]\exp(-kt)$$

where $[O_2]$ is the concentration of oxygen in solution at time t and at time 0. For the meters, the later stages of reaction follow an expression of the form

$$\ln [M] = A + k\ln(t)$$

or

$$[M] = \exp(A + k\ln(t))$$

where [M] is the concentration of the metal, A and k are constants, and t is time in seconds. Table 10 gives the measured values for the constants.

Table 10. Long-term rate constants for leaching of brass meters during stagnation.								
Meter	Age	$k_{Ox,Cu}$	$K_{Ox, Zn}$	$K_{Ox, Pb}$	$A_{Ox,Cu}$	$A_{Ox, Zn}$	$A_{Ox, Pb}$	Zn/Cu
	years							brass
1	26	0.355	0.830	0.609	1.154	-5.975	-4.845	0.054
5	0	*0.291*	*0.527*		*2.185*	*-2.778*		0.063
2	19	0.325	0.470	0.375	1.820	-2.243	-2.708	0.099
6	0	0.259	0.366	0.243	2.396	-1.066	-0.503	0.104
3	4	0.371	0.402	0.237	1.691	-1.758	-1.217	0.108
4	40	0.268	0.228	0.178	2.250	-0.496	-1.503	0.121

In this case, the rates for Zn and Pb correlate to the Zn/Cu ratio of the brass. The higher the Zn content, the slower the leaching rate of Zn and Pb from the brass (Fig. 18).
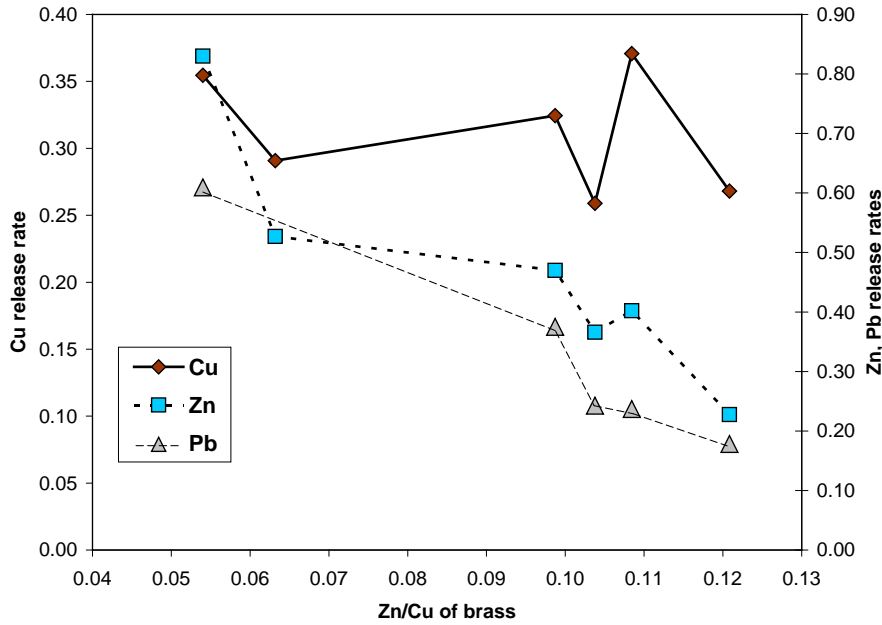

Figure 18. The rates of metal release at long stagnation times (> 5 hours), as a function of Zn content of the brass.

Copper does not follow the same behavior as Pb and Zn for either portion of the reaction. A likely reason is the presence of abundant Cu-bearing scale minerals that can dissolve independently of the oxidation of the copper metal.

Discussion of kinetic behavior

The literature on brass corrosion indicates that dezincification should increase as the Zn content of the brass increases, instead of the observation in these experiments that corrosion decreases with increasing Zn. An explanation of the results can be found in recent work by Marshakov (2005) on brass corrosion. He reports data from α-brasses of a variety of Zn contents in which the corrosion rate in stagnant water decreases with increasing Zn content, just as found in these experiments (Fig. 19, lower curve). In running water, however, the situation is reversed, with corrosion rate increasing with increasing Zn content (Fig. 19, upper curve).
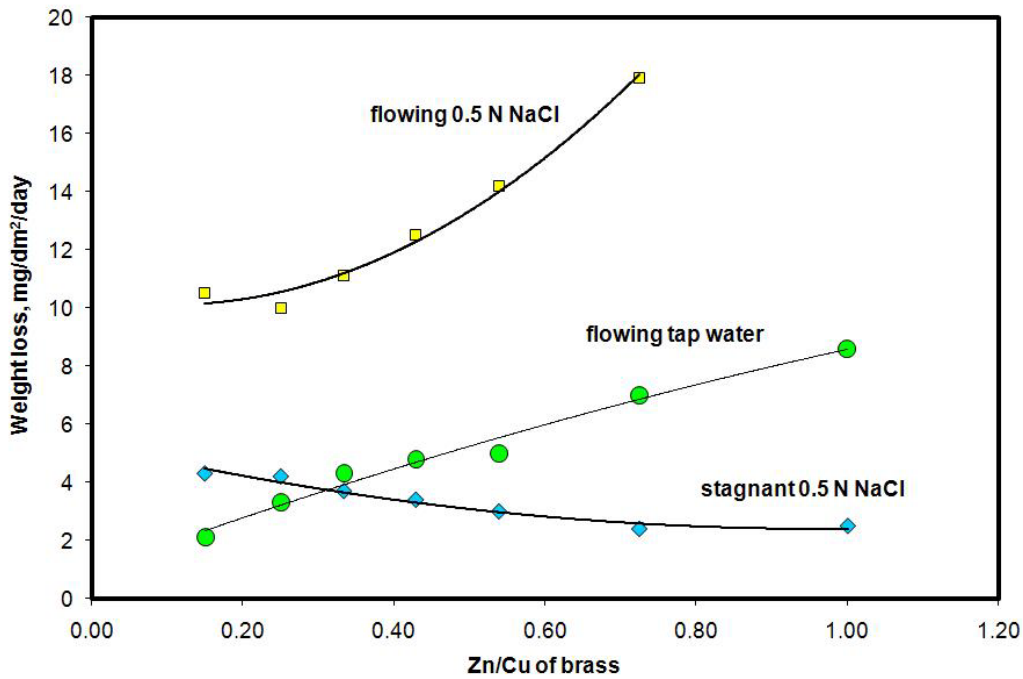

Figure 19. Corrosion rates for brass coupons as a function of Zn/Cu content of the brass. The r^2 values for the two functions are 0.982 and 0.985. Flowing 0.5 N NaCl produces similar results to the flowing tap water, but with rates about 2X higher.

The explanation for this contrast is that in the stagnant water, Cu^{2+} ions accumulate and catalyze the reaction

$$Cu\ metal + Cu^{2+} \longrightarrow 2Cu^{1+}$$
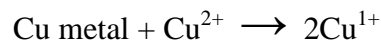
As long as oxygen remains in the water (Lytle and Shock, 2000), the cupric ions can be regenerated via

$$4Cu^{1+} + 4H^+ + O_2 \longrightarrow 4Cu^{2+} + 2H_2O$$
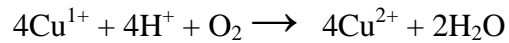
and the reaction continues. See Rehan et al. (2001) for a discussion of these reactions.

The higher Cu brasses (those with lower Zn/Cu ratios in Fig. 19) release more Cu to solution in short stagnation cycles; therefore they corrode more quickly than lower Cu brasses. In flowing water, on the other hand, the buildup of the copper ions in solution is precluded, and the autocatalytic effect does not occur. In this case, the corrosion rate is controlled by the diffusion of Zn from the metal, which increases with increasing Zn content. This effect produces the relationship shown by the upper curve in Fig. 19.

References

Cardew, P.T., 2006, Development of a convective diffusion model for lead pipe rigs operating in laminar flow: Water Research v. 40, p. 2190-2200.

Crank, J., 1956, The Mathematics of Diffusion: Oxford, the Clarendon Press, 347 pp.

Dudi, A., Schock, M., Murray, N., and Edwards, M., 1997, Lead leaching from inline brass devices: a critical evaluation of the existing standard: Journal of the American Water Works Association, 97-8, p.66-78.

Lytle, D.A. and Shock, M.R., 2000, Impact of stagnation time on metal dissolution from plumbing materials in drinking water: Journal of Water Supply: Research and Technology – Aqua, 49.5, p. 243-257.

Marshakov, I.K., 2005, Corrosion resistance and dezincing of brasses: Protection of Metals, v. 41, p. 2305-210.

Merkel, T.H., Gross, H-J., Werner, W., Dahlke, T., Reicherter, S., Beuchle, G., and Eberle, S.H., 2002, Copper corrosion by-product release in long-term stagnation experiments: Water Research, v. 36, p. 1547-1555.

Rehan, H.H., Al-Moubarak, N.A., and Al-Rafai, H.A., 2000, A model for prolonged dezincification of α-brasses in 3 % sodium chloride buffer solutions at different pH values: Materials and Corrosion, v. 52, p. 677-684.

Valcarce, M.B., de Sánchez, S.R., and Vázquez, M., 2005, Localized attack of copper and brass in tap water: the effect of *Pseudomonas*: Corrosion Science, v. 47, p. 795-809.